Applied Catalysis B: Environmental 136–137 (2013) 278–286

Contents lists available at SciVerse ScienceDirect

Applied Catalysis B: Environmental

journal homepage: www.elsevier.com/locate/apcatb

Fabrication of novel SnO_2-Sb/carbon aerogel electrode for ultrasonic electrochemical oxidation of perfluorooctanoate with high catalytic efficiency

Hongying Zhao[a,b], Junxia Gao[a,c], Guohua Zhao[a,b,*], Jiaqi Fan[a], Yanbin Wang[a], Yujing Wang[a]

[a] Department of Chemistry, Tongji University, 1239 Siping Road, Shanghai 200092, PR China
[b] Key Laboratory of Yangtze River Water Environment, Ministry of Education, Tongji University, 1239 Siping Road, Shanghai 200092, PR China
[c] High-Tech Induastrial Development Zone Branch of Jining Environmental Protection Bureau, 116 Wutaizha Donglu, Jining 272000, PR China

ARTICLE INFO

Article history:
Received 13 September 2012
Received in revised form
21 December 2012
Accepted 1 February 2013
Available online 19 February 2013

Keywords:
Sb-doped SnO_2
Carbon aerogel electrode
Electrochemical oxidation
Ultrasonic irradiation
Perfluorooctanoate

ABSTRACT

A novel SnO_2-Sb/CA electrode, possessing high surface area, strong adsorption capacity, good electrical conductivity and electrocatalytic activity, was firstly proposed for ultrasonic electrochemical oxidation (US-EC) of persistent high concentration perfluorooctanoate (PFOA) in this study. The optimal calcination temperature for sinking micro-sized SnO_2-Sb particles existed on the surface of CA into the structure of CA as nanoparticles was 600 °C. Its application on degrading PFOA (60 mL of 100 mg L^{-1}) exhibited efficient electrocatalytic performance. After 5 h electrolysis, over 91% of PFOA was degraded with a first-order kinetic constant of 0.52 h^{-1} and over 86% TOC removal was achieved, while 47% PFOA removal and 33% TOC removal were obtained in traditional electrochemical (EC) process. The main role of determining the decomposition efficiency, i.e., the mass transport, hydroxyl radical (·OH) generation and electrode surface reaction, were greatly enhanced in US-EC system. Additionally, the generated intermediates existing on electrode surface and in solution were separately detected after different electrolysis time and the proper mechanism for efficient removing PFOA in US-EC process was investigated in detail. At early reaction stage (<0.5 h), the intermediate products on SnO_2-Sb/CA surface were $C_5F_{11}COO^-$, $C_4F_9COO^-$, $C_3F_7COO^-$, $C_2F_5COO^-$, CF_3COO^-, while in solution were $C_5F_{11}COO^-$, $C_4F_9COO^-$, $C_3F_7COO^-$. At late reaction stage (>5 h), the intermediates either on electrode surface or in solution became the same including $C_5F_{11}COO^-$, $C_4F_9COO^-$, $C_3F_7COO^-$.

1. Introduction

Over the past years, perfluorooctanoic acid ($C_7F_{15}COOH$, PFOA), one of perfluorinated compounds, has been produced in large amounts and widely applied in industries and medical activities due to its hydrophobic and oleophobic properties [1,2]. The extensive use of PFOA resulted in its detection in various environmental matrices including sediments, domestic sludge, water and biotic samples such as human sera, bird liver, fish blood, which pose a risk to human health. Hence it is important and urgent to degrade PFOA to harmless species [3].

Recently, various methods such as photocatalysis [4–6], sonolysis [7], and chemical oxidation by periodate (IO_4^-) [8] or persulfate ($(S_2O_8^{2-})_6$ [9] are investigated as oxidative technique to remove PFOA from the environment, and the reduction by using zero-valent iron [10], thermolysis [11] are also reported. However, due to the strong bond energy of the C—F bond (116 kcal mol^{-1}) and a high reduction potential (E_0 = 3.6 V), PFOA is extremely stable to most chemical and thermal destruction technologies.

Compared to the above methods, electrochemical oxidation (EC) technique has become a promising process since its strong oxidation performance, mild treatment condition and environmental compatibility. It has been demonstrated that Sb-doped SnO_2 (denoted as SnO_2-Sb) is of good electrocatalytic activity among so many catalyst species, which is especially suitable for the electrocatalytic oxidation of organic pollutants [12,13]. Previous studies also showed that SnO_2-Sb-based materials have higher oxidation efficiency for phenol, quinone, aromatic compounds, nitrogen pollutants, and the toxic intermediates that can be fast decomposed [14,15]. In addition, SnO_2-Sb itself possesses higher oxygen evolution potential (1.8 V, vs SCE)[15]. So, similar as boron doped

* Corresponding author at: Tongji University, Department of Chemistry, 1239 Siping Road, Shanghai 200092, China. Tel.: +86 21 65988570; fax: +86 21 65982287.
E-mail address: g.zhao@tongji.edu.cn (G. Zhao).

0926-3373/$ – see front matter © 2013 Elsevier B.V. All rights reserved.
http://dx.doi.org/10.1016/j.apcatb.2013.02.013

diamond (BDD)[16,17] and PbO_2 electrodes [18], it has been widely considered as one of the most suitable electrodes in the purification of refractory organic pollutants.

Whereas, till now titanium seems to be a preferable choice as a substrate for deposition SnO_2-based electrocatalysts in case comparing to expensive BDD, tantalum, niobium, tungsten substrates and/or to brittle silicon substrate with poor conductivity [19]. But the service life of Ti electrode is relatively short and the active surface area is quite low, which may limit the catalytic performance of SnO_2-based electrocatalyst [20]. Herein, searching for an inexpensive electrode, owning high surface area and potential for industrial application, for efficient degrading PFOA at mild condition is still a challenge.

Carbon aerogel (CA), representative of novel porous electrode materials, presents three-dimensional network structure, high surface area and good electrical conductivity, which could be a promising substrate during the EC process. In addition, these properties may enhance the electrosorption capacity of electrode and improve the oxidation performance of EC method. Thus, it would be very reasonable to suppose the active sites on electrode surface would be increased and the efficiency of electrochemical oxidation would be improved by choosing CA as substrate to disperse SnO_2-Sb electrocatalysts.

Although the degradation efficiency can be improved by fabricating novel and active electrode to enhance its adsorption capacity and electrochemical oxidation ability, the combination of treatment techniques [21,22] are also been received considerable attentions for the treatment of wastewater especially with persistent organic pollutants. Ultrasonic irradiation (US) of aqueous solution is well known for yielding sonochemistry via cavitation. The ultrasonic pressure waves interact with the cavitated bubbles, causing high velocity radial oscillations and produce bubble vapor and interface temperatures respectively near 4000 K and 1000 K. This cavitation phenomenon can bring physical effect which can clean electrode surface and improve mass transport and cause chemical effect which can produce active substances such as hydroxyl free radicals (•OH) [23,24].

Based on the above consideration, the degradation of high concentration PFOA in ultrasonic electrochemical oxidation system with novel SnO_2-Sb/CA electrode were proposed and deeply studied. The influence of calcination temperature on the interaction between SnO_2-Sb electrocatalyst and CA electrode substrate was evaluated. Additionally, the surface and electrochemical properties of obtained electrode were characterized with comprehensive physicochemical techniques. The main parameters for determining the PFOA degradation efficiency in US-EC were discussed in detail expecting to explain the effects between electrode catalysts and US. The identification of intermediates was further conducted and then a possible corresponding mechanism was proposed.

2. Experimental

2.1. Preparation and characterization of SnO_2-Sb/CA electrode

Resorcinol, formaldehyde, sodium carbonate, acetone, ethyl alcohol, sodium hydroxide, hydrochloric acid, tin(IV) chloride, antimony(III) chloride and tristyrenephenol polyoxyethylene ether were obtained from Aladdin Co., China and PFOA was obtained from Sigma. All of the chemicals were reagent grade and used without further purification. The carbon aerogel (CA) was prepared through sol-gel formation, solvent exchange, ambient pressure drying and pyrolysis, which according to a modified ambient drying technique [25,26]. The detailed preparation process and schematic illustration was further presented in the following discussion part. The composite SnO_2-Sb/CA electrode was synthesized through a typical sol–gel method. Briefly, 17.53 g $SnCl_4{\cdot}5H_2O$, 0.60 g $SbCl_3{\cdot}2H_2O$ and 0.1 g tristyrenephenol polyoxyethylene ether were dissolved into 80 mL dehydrated ethanol with constant stirring. Then concentrated hydrochloric acid was slowly dropped into the above mixture to form clear solution. The clear solution was stirred for 24 h and then put it aside for 8 h to form the metal ion containing solution (S1). CA was firstly dipped into S1 solution for 30 min, then dried in the oven at 90 °C for 8 h, and took out from oven to naturally cool down to room temperature, all of which were repeated for 5 times. The resulting CA containing the Sn and Sb metal ion was then calcined in N_2 for 2 h to obtain SnO_2-Sb/CA electrode. The heating rate was 1.5 °C/min from 30 °C to 400, 500, and 600 °C, respectively.

The surface area and pore size of CA and SnO_2-Sb/CA were measured by nitrogen adsorption at 77 K on a Micromeritics 3000 apparatus after heat treatment under vacuum at 573 K for 3 h. The X-ray diffraction (XRD) measurements were carried out on a Rigaku–D/max2550 powder diffractometer with Cu Kα radiation (at 40 kV, 30 mA over the 2θ range 3–80 °C). The morphology and microstructure were characterized by using scanning electron microscopy (SEM, Hitachi-S4800).

Accelerated servicelife test were performed by anodic polarization of the different electrodes at 100 mA cm^{-2} in a 0.1 M H_2SO_4 solution to access the service lifetime [27,28]. The anode potential was measured as a function of time, considering that the electrode is deactivated when the potential increases 5 V from its initial value.

2.2. Electrochemical property test

Electrochemical measurements were performed on a CHI 660c electrochemical workstation (CHI Co.) using a conventional three-electrode cell system. The SnO_2-Sb/CA and SnO_2-Sb/Ti electrode were employed as electrode. A SCE served as the reference electrode and a Pt wire as the counter electrode. All the potentials were referred to SCE unless otherwise stated in this work. Electrochemical impedance spectrum (EIS) was tested in the electrolyte consisting 5 mM $[Fe(CN)_6]^{3-}/[Fe(CN)_6]^{4-}$ by means of alternative current (AC) impedance with the frequency ranging from 1×10^5 to 1×10^{-3} HZ and an impedance amplitude of 5 mV. The amount of deposited Sb-doped SnO_2 was determined by weighing the electrode before and after the Sb-doped SnO_2 deposition using a balance with a 0.1 mg [29].

2.3. Electrochemical degradation of PFOA with and without ultrasound

EC oxidation of PFOA was carried out in a cylindrical single-compartment cell with jacketed cooler to maintain constant temperature, using SnO_2-Sb/CA or SnO_2-Sb/Ti electrode, with an immersed area of 5 cm^2, as electrode. A titanium foil with the same area was used as anode and the interelectrode gap was 1 cm. The current density was controlled at 20 mA cm^{-2}. A 100 mg L^{-1} PEOA solution in 0.1 M Na_2SO_4 was degraded. The volume of solution was 60 mL in each run. US-EC degradation was carried out by a US probe immersed in solution at the frequency of 33 kHz, with the power of 50 W, and other conditions were the same as those in EC process. In order to avoid temperature of EC and US-EC processes was kept at 20 °C by circulating-water.

2.4. Analytical procedure

The concentration of PFOA during the US-EC and EC oxidation process was analyzed by reversed-phase HPLC chromatography (Agilent HP 1100, Agilent Corporation, USA) at room temperature equipped with Agilent AQ-C18 column (4.6 mm × 150 mm × 5 μm) and selected photodiode detector at $\lambda = 275$ nm. The mobile

phase was methanol/a buffer (pH 2.3) of 1:2 (v/v) 50 mmol NaH_2PO_4/50 mmol H_3PO_4 = 30:70 at 0.4 ml min^{-1}. In each case, 20 μL aliquots were injected into HPLC.

GC/MS (Agilent 6890/5973 N, Hp-1, L = 30 m, Ø = 0.25 mm, e = 0.5 μm) was also used for the volatile intermediates analysis. The column temperature program was: 323 K (5 min), 323–553 K (10 K min^{-1}, hold time: 5 min). The concentrations of F^- in the solution produced during the reactions were detected by a F^- selective electrode. TOC was measured by TOC analyzer (TOC-Vcpn, Shimadzu, Japan).

The hydroxyl radicals were determined with a simple and sensitive method which has been widely reported in the literatures [30–32]. The proposed method employed the reaction between hydroxyl radicals and dimethyl sulfoxide (DMSO). Formaldehyde firstly was quantitatively generated, which then reacted with 2,4-dinitrophenylhydrazine (DNPH) to form the corresponding hydrazine (HCHO-DNPH) and further analyzed by HPLC (Agilent HP 1100, Agilent). An Agilent Zorbax Eclipse XDB-C18 column (150 mm × 4.6 mm × 5 μm) was used at room temperature and with selected UV detector at λ = 355 nm. To perform the isocratic elution at a flow rate of 1.0 mL min^{-1}, a mixture of methanol and water (60:40, v/v) was used as mobile phase. Specially, the determination of hydroxyl radicals was carried out in a divided system with 250 mM DMSO.

The diffusion coefficient (D) of PFOA on the electrode surface are determined by the one-step chronocoulometry method in EC and US-EC process, respectively [33,34]. In which the Cottrell formula is used.

$$Q = nF\,G + Q_{dl} + \frac{2nFAC_{ox}^{0}D^{1/2}t^{1/2}}{\pi^{1/2}} \quad (1)$$

where Q is the total amount of charge (C cm^{-2}), A is the real area of electrode (cm^2), C_{ox}^{0} is the concentration of component in a solution (mol cm^{-3}), D is the diffusion coefficient of component in water (cm^{-2} S^{-1}), t is time (s). G is the reaction amount of component at the electrode surface (mol cm^{-2}), Q_{dl} is the number of coulombs required for double-layer charging (C cm^{-2}), and n is the number of electrons per pollutant molecule transferred in the oxidation reaction on the electrode.

3. Results and discussion

3.1. The fabrication, structural and electrochemical properties of novel SnO_2-Sb/CA electrode

Fig. 1 illustrates the preparation process of this novel SnO_2-Sb/CA electrode. Firstly, resorcinol, formaldehyde, deionized water and sodium carbonate were mixed with a fixed molar ratio to form a homogeneous solution. Secondly, the mixture was casted into a cuboid reactor and then separately cured at 30, 50 and 90 °C for

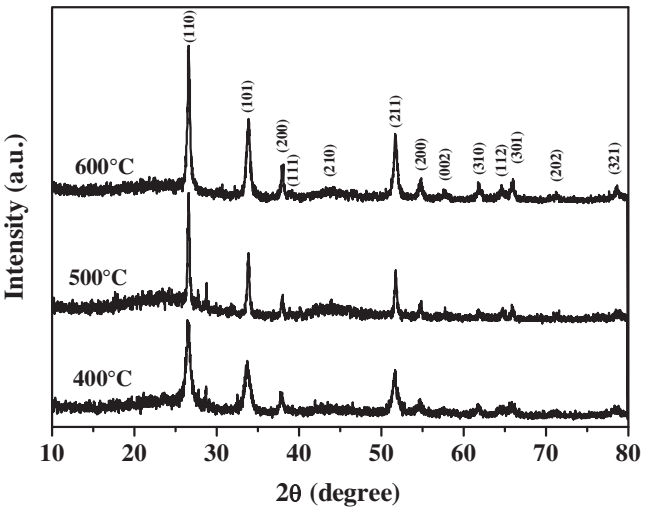

Fig. 2. X-ray diffraction (XRD) patterns of SnO_2-Sb/CA electrodes calcined at different temperatures.

resulting in organic wet gel (RF). Thirdly, the RF gel was dried in solvent exchange process under ambient condition and then calcined at 950 °C for 4 h in argon atmosphere to convert to CA. Finally, CA was dipped into SnO_2-Sb containing solution, and then dried in oven. All these procedures were repeated for 5 times to obtain Sb-SnO_2 doped CA electrode precursor, which would be calcined at desired temperatures through typical sol–gel methods described in Section 2.

Since SnO_2-Sb/CA electrode possesses promising electrocatalytic ability, it is very important to optimize its fabrication conditions. The heat-treating temperature plays an important role on the structure and crystallinity of as-synthesized electrodes [35], which is related with its electrocatalytic performance. Therefore, a detailed analysis of the grain growth behavior of crystal SnO_2-Sb and its interactions between substrate CA was carried out for the following cognition of catalytic activity.

The composition and crystal structure of SnO_2-Sb/CA electrodes calcined at different temperature were examined by XRD analysis. As presented in Fig. 2, typical diffraction peaks characteristic of pure SnO_2 were in excellent accordance with the tetragonal rutile structure (JCPDS 41-1445) for sample sintered at 400 °C, which belongs to the space group of $P4_{2/mnm}$ (136), and its lattice parameters were calculated as $a = b = 4.736(4)$ Å and $c = 3.187(6)$ Å [36]. No impurity peaks were detected, which shows that the products are pure phase. With increasing calcination temperature to 500 and 600 °C, the intensity of peaks were increased. However, the half-peak widths did not show a remarkable change. This means that, increasing calcination temperature did not cause a

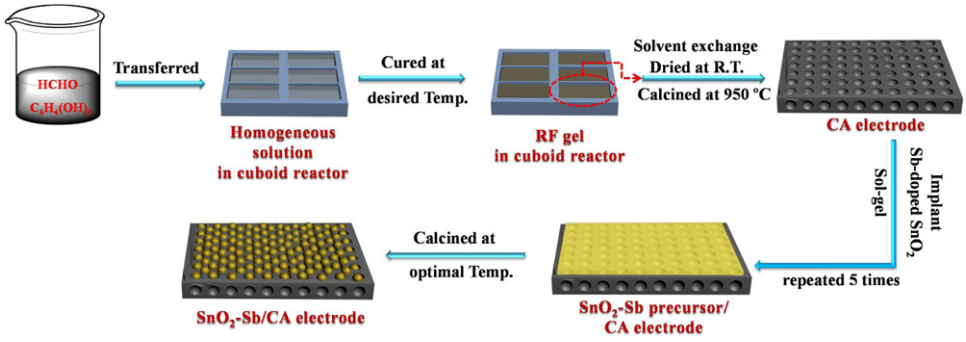

Fig. 1. Schematic illustration for fabrication novel SnO_2-Sb/CA electrode.

notability increase in the crystal size, only the crystallinity was enhanced. From the XRD patterns, no diffraction peaks of metallic Sn were obtained, possibly due to the traces amount of Sn and/or the fine dispersion of Sn when heat-treated lower than 700 °C [35]

The SEM images of SnO_2-Sb/CA electrodes, as presented in Fig. 3, further revealed the effect of calcination temperature on the formation and morphology of SnO_2-Sb. As depictured in our previous work [25] CA possessed smooth surface and excellent network structure, as shown in Fig. 3A. With the addition of SnO_2-Sb and calcined at 400 °C, the structure of CA still remained the same (see Fig. 3B on the right), and a slight of micropolyhedral SnO_2 particles appeared on the surface of CA (see Fig. 3B on the left). However, as shown in Fig. 3B on the right, most of SnO_2 were presented as nanoparticles, which were well dispersed on surface of CA and filled the pore of CA. With rising the calcination temperature to 500 °C, it is interesting to found that micropolyhedral SnO_2 seemed to be dissolved with reduced size and irregular shape. Meanwhile, the amount of nanoparticle SnO_2, exhibited in Fig. 3C on the right, was increased. In another word, high calcination temperature resulted in the sinking of SnO_2 into the structure of CA, favoring the interactions between SnO_2 particles and CA support. This observation was further demonstrated with increasing calcination temperature to 600 °C. All micron-sized SnO_2 were completely disappeared (Fig. 3D on the left) and correspondingly converted to the well dispersed and increased white nanoparticles (Fig. 3D on the right). According to the previous studies, the optimal calcination temperature for

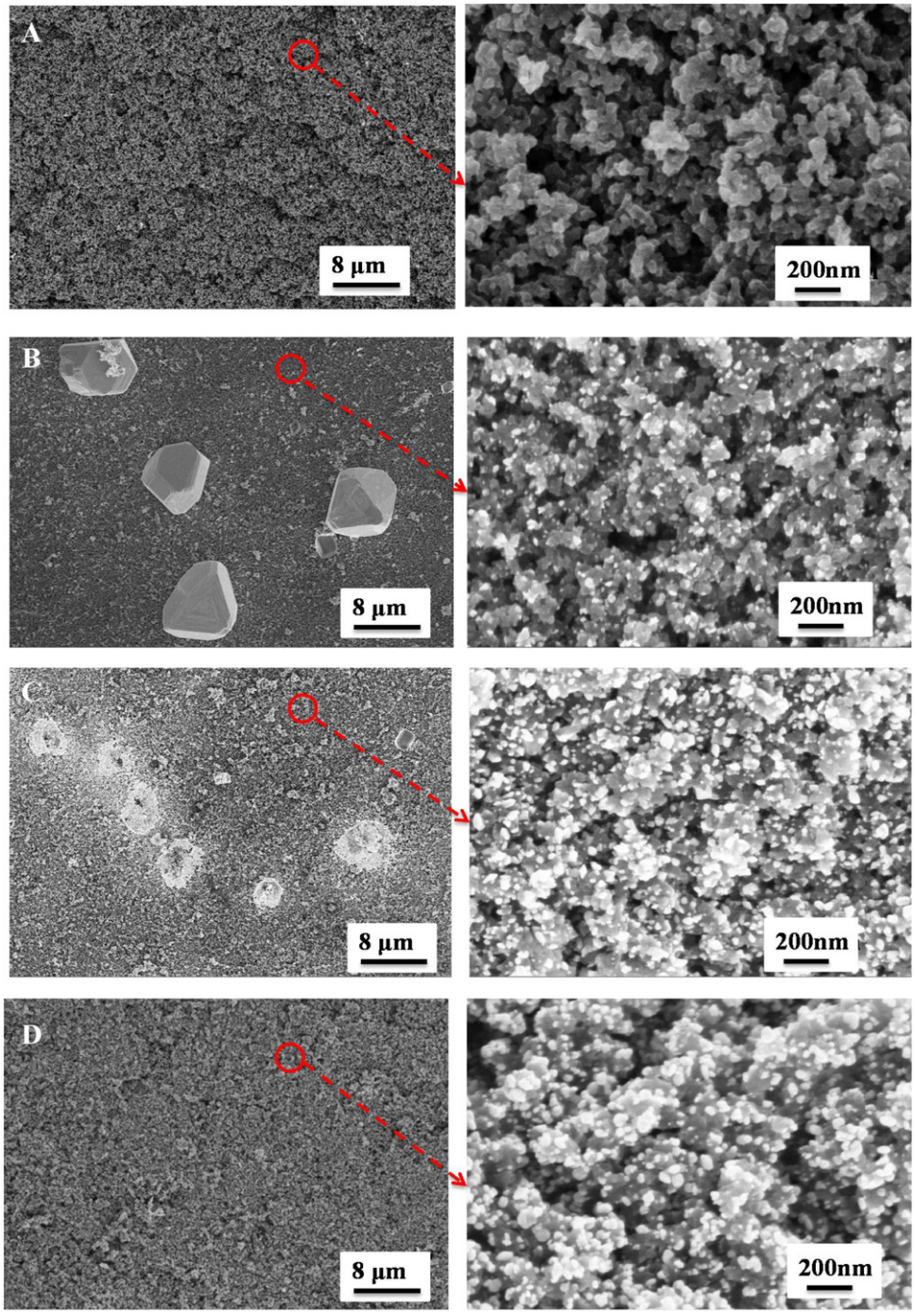

Fig. 3. SEM images of SnO_2-Sb/CA electrodes calcined at different temperatures: (A) 400 °C, (B) 500 °C, (C) 600 °C.

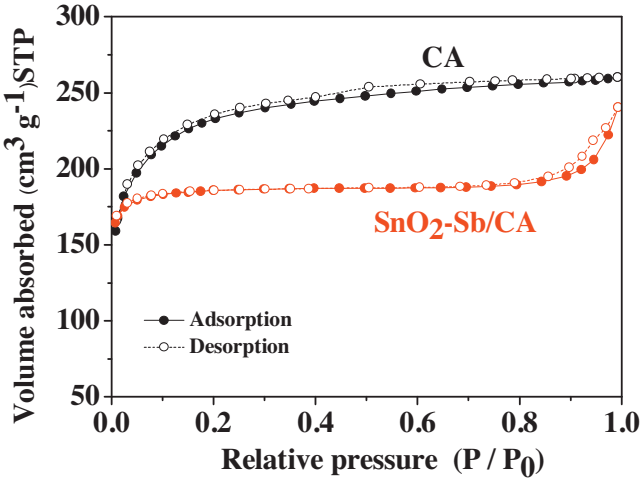

Fig. 4. N2 adsorption-desorption isotherms of CA and SnO_2-Sb/CA electrode calcined at 600 °C.

SnO_2-based electrode was around 550 °C [37,38]. The electrode at this temperature had higher oxygen evolution potential and electrocatalysis ability, and stability of electrode. Moreover, CA would reduce SnO_2 to metallic Sn under high heat treatment (>700 °C) due to the reducibility of substrate CA [35]. These features, to some extent, revealed that calcination temperature of 600 °C would be the most suitable for gaining the stronger electrochemical capacity, higher coverage of crystal SnO_2 and obtaining better interaction between SnO_2 and CA. Therefore, we choose SnO_2-Sb/CA electrodes calcined at 600 °C for the further analysis in the whole text.

Research on the structural and electrochemical characteristic of electrode is helpful in selecting electrode materials for high-efficiency EC process, thus the comprehensive characterization were carried out for the prepared electrodes. The N_2 adsorption-desorption isotherms of pure CA and SnO_2-Sb/CA electrode are depicted in Fig. 4. The sharp of the isotherm for CA, similar to type I, shows a typical isotherm for microporous materials. The hysteresis (type H3 loop) in the isotherm can be observed for SnO_2-Sb/CA electrode, which is often associated with narrow slit-like pores [39]. This observation would be suggested that some chemical precursors penetrated into microspores of CA during the immersion process and new porous structures are roughly replicated in the CA samples after the calcination treatment. In addition, the detailed BET surface area, porosity data, resistance and electrochemical impedance are summarized in Table 1. After loading SnO_2-Sb, the BET surface area of CA was decreased from 744 to 613 $m^2\,g^{-1}$ and the micropores volume was declined from 0.277 to 0.259 $cm^3\,g^{-1}$. That is to say, the SnO_2-Sb/CA electrode, a porous electrode with excellent adsorptive property, still maintains high BET surface area and large microspores volume especially comparing to commercial active carbon (S_{BET}: 400–800 $m^2\,g^{-1}$; V_{micro}: 0.2–0.4 $cm^3\,g^{-1}$).

It is well known that CA is an excellent conductive material. The measured resistance of pure CA is 2.5 $\Omega\,cm^{-1}$, and the corresponding electrochemical impedance is 7.8 Ω (as shown in Table 1). This is why CA is regarded as a favorable substrate in electrochemical process. When SnO_2-Sb was loaded on CA, the measured resistance and electrochemical impedance of this composite electrode was slightly increased to 15 $\Omega\,cm^{-1}$ and 20 Ω, respectively, suggesting the persisted good conductivity for SnO_2-Sb/CA electrode. The observation indicated that CA is still exposed, with some SnO_2-Sb particles inside the pores and some discontinuous film of SnO_2-Sb on CA surface (Fig. 2). Thus, the electron transfer on the interface of CA and solution is not seriously impeded with the addition of SnO_2-Sb. Additionally, the electrochemical effective surface area of SnO_2-Sb/CA was calculated based on the equation of $i_p = (2.69 \times 10^5) n^{\frac{3}{2}} A D_0 C_0 v^{\frac{1}{2}}$ by using $K_3[Fe(CN)_6$ as model complex (the diffusion coefficient D_0 of $K_3[Fe(CN)_6$ is $7.6 \times 10^{-6}\,cm^2\,s^{-1}$) [40],where i_p is peak current (A); A is the effective surface area (cm^2); n: number of electron transfer reaction; C_0: concentration of $K_3[Fe(CN)_6$ solution; v: scan rate ($V\,s^{-1}$). The effective surface area was 5.25 times of its geometric surface area. That is to say, SnO_2-Sb/CA electrode exhibited high electrochemical catalytic properties.

Table 1
Surface area, porosity data, load capacity, resistance and electrochemical impedance of CA and SnO_2-Sb/CA electrodes.

Properties	CA	SnO_2-Sb/CA
S_{BET} ($m^2\,g^{-1}$)	744	613
Micro pore volume ($cm^3\,g^{-1}$)	0.277	0.259
SnO_2-Sb load capacity ($mg\,cm^{-2}$)	0.0	2.72
Resistance ($\Omega\,cm^{-1}$)	2.5	15
Electrochemical impedance (Ω)	7.8	20.0

3.2. Strong electrochemical oxidation ability and efficient catalytic degradation performance on SnO_2-Sb/CA electrode with ultrasonic irradiation

Based on the above results, we can know that the fabricated SnO_2-Sb/CA with high surface area was a promising electrode for removing quite stable and environmental persistent PFOA. In order to confirm that SnO_2-Sb/CA electrode has excellent electrocatalytic ability, common SnO_2-Sb/Ti electrode is selected as reference in this work.

As shown in Fig. 5, the current density for SnO_2-Sb/Ti electrode was improved from 4.1 to 22.4 $mA\,cm^{-2}$, with the increasement of 18 $mA\,cm^{-2}$, after adding PFOA into the solution, while the increasement for SnO_2-Sb/CA electrode was 57 $mA\,cm^{-2}$, raising from 11.6 to 68.6 $mA\,cm^{-2}$. The enhancement of current density with the addition of PFOA was attributed to the PFOA electrocatalytic oxidation on the electrode. Moreover, it is very clearly to note that the current density of SnO_2-Sb/CA was always greatly higher than SnO_2-Sb/Ti electrode especially in case of PFOA existing. These results further revealed that SnO_2-Sb/CA electrode possessed very high electrocatalytic performance, mostly due to the porous structure and high surface area of substrate CA as well as the properties of electrocatalyst, i.e., the distribution and amounts of SnO_2-Sb. As shown in Table 1, the loading amount of Sb-doped SnO_2 on CA is around 2.72 $mg\,cm^{-2}$, while on Ti substrate is around 0.92 $mg\,cm^{-2}$

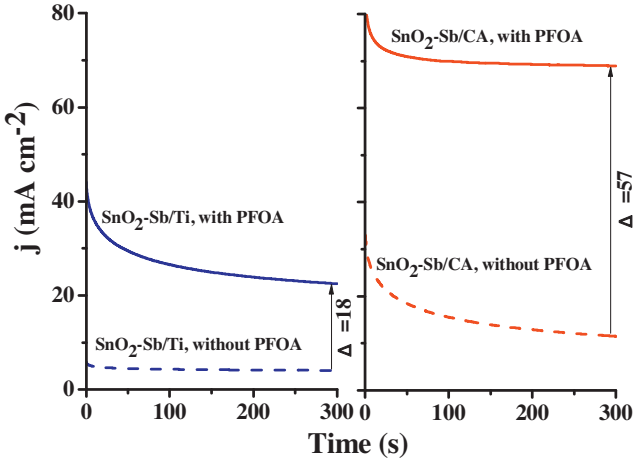

Fig. 5. Amperometric i–t curves in the Na_2SO_4 solution at applied potentials of 3.0 V with and without 100 $mg\,L^{-1}$ PFOA solution.

(cm^{-2} means per geometric area of electrode). In fact, the electrode's electrochemical ability could be effectively improved by increasing electrocatalyst load [41,42]. The obviously enhanced load amount of SnO_2-Sb on CA was also attributed to the three-dimensional porous structure and large specific surface area of CA. Moreover, since the above mentioned properties of CA, SnO_2-Sb particles were dispersed very well on the surface of substrate CA even with very high amounts (see Fig. 3D), while SnO_2-Sb with low amount were aggregated together on Ti substrate (not shown). This phenomenon, to some extent, suggests that SnO_2-Sb/CA electrode possess more active sites in heterogeneous catalytic reaction, which is a potential reason for higher current value and enhanced electrochemical performance.

According to the above results that CA has the potential of enhancing adsorption capacity both for pollutants and electrocatalysts, and improving electrocatalysis ability of SnO_2-Sb, it would be very interesting to further develop degradation efficiency based on this novel electrode by combing ultrasonic irradiation with traditional electrochemical oxidation process. The degradation efficiency of PFOA with different electrode in EC and US-EC process was evaluated in Fig. 6A–C. The removal of PFOA was improved with increasing the electrolysis time for all electrodes (see Fig. 6A). For pure CA, the removal of PFOA at 5 h was achieved to 18.5%, possibly due to the high surface area and strong electroadsorption ability of CA. While for SnO_2-Sb/CA electrode, at 5 h, the removal of PFOA was 47.1% in EC process, which was respectively increased 220% and 125% compared with SnO_2-Sb/Ti electrode (14.7%) and pure CA (18.5%). Obviously, the degradation efficiency on electrode substrate CA is a much higher than Ti. The obviously enhancement catalytic performance of SnO_2-Sb/CA electrode was possibly due to the three-dimensional porous structure and large specific surface area of CA, which not only possesses strong adsorption ability but also can enhance the amount of SnO_2-Sb and improve the dispersion of SnO_2-Sb on substrate CA. After combing ultrasound, the removal of PFOA at 5 h for SnO_2-Sb/CA and SnO_2-Sb/Ti in US-EC process was obviously increased to 91.3% and 26.0%, respectively. That means the degradation efficiency was greatly improved with the aid of ultrasonic irradiation especially for SnO_2-Sb/CA electrode. However, only 4.4% PFOA was degraded with solo ultrasound (not shown), which due to the produced sonochemistry via cavitation [43]. Whereas, this results suggested that the enhanced efficiency was most possible owing to the synergistic function between ultrasonic electrochemical oxidation process and SnO_2-Sb/CA electrode catalyst not only due to the sonochemical effect.

The data for PFOA concentration decay were further analyzed by kinetic equations. Good linear plots were obtained when fitted to a pseudofirst-order reaction, as shown in Fig. 6B. The pseudofirst-order rate constant (k) for SnO_2-Sb/CA in US-EC systems was $14.5 \times 10^{-5}\ s^{-1}$ increased by 306% comparing to solo EC system ($k = 3.57 \times 10^{-5}\ s^{-1}$). For pure CA, the k value was increased 67% from $1.15 \times 10^{-5}\ s^{-1}$ in EC system to $1.92 \times 10^{-5}\ s^{-1}$ in US-EC systems, while for SnO_2-Sb/Ti electrode, the k value was increased 89% from $0.88 \times 10^{-5}\ s^{-1}$ to $1.67 \times 10^{-5}\ s^{-1}$ with the aid of US, implying that US-EC oxidation with SnO_2-Sb/CA electrode was an efficient and promising method to decompose PFOA.

The total organic carbon (TOC) in reaction solution was measured as an indicator for the organic mineralization at different time intervals. Fig. 6C plots the TOC removal in 5 h for SnO_2-Sb/CA and SnO_2-Sb/Ti electrodes both in EC and US-EC processes. Obviously, SnO_2-Sb/CA electrode in US-EC system exhibited extremely high mineralization ability in this work. In this case the TOC removal was up to 86% at 5 h, which was much higher than that of 33% for SnO_2-Sb/CA in EC, 17% and 8% for SnO_2-Sb/Ti respectively in US-EC and EC system at the same electrolysis time.

The concentration of F^- (C_{F^-}) was also detected during the degradation process for both electrodes with and without US. As

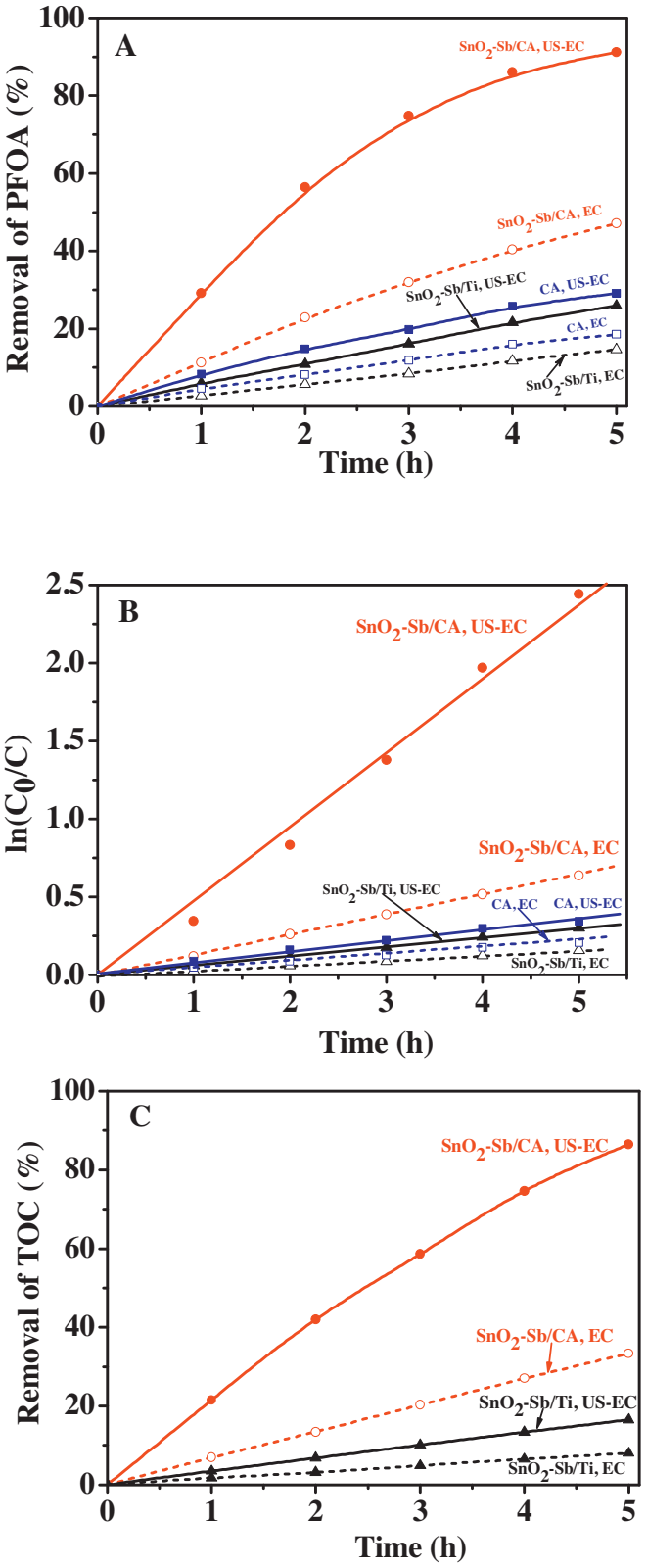

Fig. 6. Degradation efficiency of 100 mg L^{-1} PFOA solution with different electrodes in EC and US-EC processes. (A) Removal of PFOA, (B) Variation of $\ln(C_0/C)$ for the treatment of PFOA, and (C) Removal of TOC.

shown in Fig. 7, C_{F^-} continued to rise with increasing electrolysis time for each system. For SnO_2-Sb/CA, at 5 h, C_{F^-} was 1.2 mM and 2.9 mM in EC and US-EC system, respectively. Obviously, ultrasonic irradiation improved the removingefficiency for F^-, to some extent,

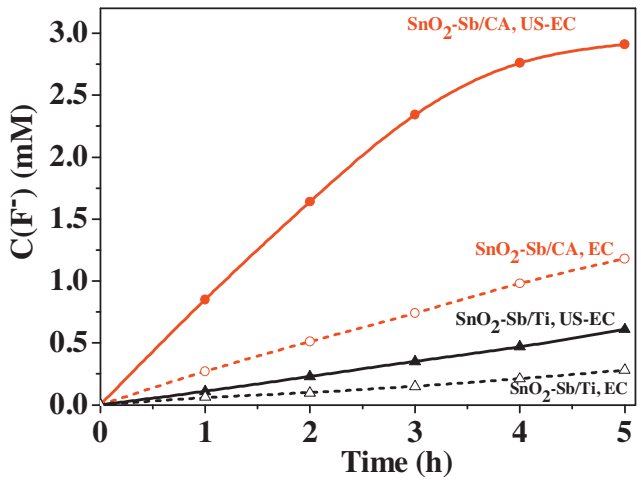

Fig. 7. Evolution of fluorine ions during the degradation of 100 mg L^{-1} PFOA solution with different electrodes in EC and US-EC processes.

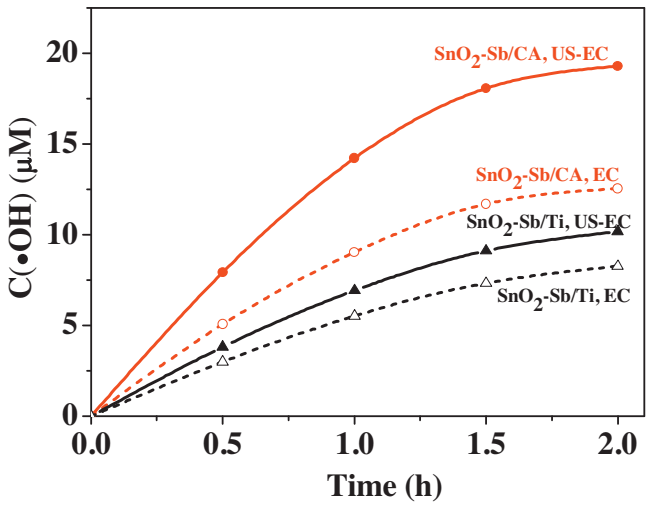

Fig. 8. The concentration of generated hydroxyl radical with SnO_2-Sb/CA and SnO_2-Sb/Ti electrodes in EC and US-EC processes.

was equivalent to enhance the mineralization ability. However, according to amount of degraded PFOA (obtained in Fig. 6A), the theoretical C_{F^-} could be 1.7 mM for EC and 3.3 mM for US-EC system, higher than the real C_{F^-} value in solution. The most possible reason can be explained by the incomplete defluorination of PFOA during the degradation process and some generated intermediates were still fluorinated compounds. For SnO_2-Sb/Ti electrode, the similar tendency was obtained. The recovery of fluorine was 0.3 and 0.6 mM at 5 h respectively in EC and US-EC system, which was lower than the theoretical value corresponding to PFOA decomposition. Nevertheless, the amount of degraded F^- with SnO_2-Sb/CA was around five times higher than SnO_2-Sb/Ti electrode, indicating the excellent electrochemical catalysis performance of SnO_2-Sb/CA.

All of these observations demonstrated the excellent degradation and mineralization capability of SnO_2-Sb/CA in US-EC process, in which the enhancement of US was much more obviously than on SnO_2-Sb/Ti electrode. Hence, it would be meaningful to investigate how US generates positive effects on electrochemical ability of SnO_2-Sb/CA electrode. Based on the above observation, we can clearly to say that SnO_2-Sb/CA electrode possess certain adsorption capacity, resulting in the part removal of pollutants. Nevertheless, •OH is a crucial parameter for understanding the degradation efficiency of electrochemical oxidation. In electrochemical oxidation system, the generated hydroxyl radicals come from the oxidation of water molecules through the following reaction: $M + H_2O \rightarrow M(^\bullet OH) + H^+ + e^-$, which depends strongly on the nature of used electrode material. In another word, the amount of generated hydroxyl radicals, to some extent, can reflect the activity of electrode. Furthermore, •OH radical has a high standard potential ($E^0(^\bullet OH/H_2O) = 2.80$ V versus SHE) and it is the second most strong oxidizing species, next to fluorine [44–46]. The generated •OH radical can be used to efficiently oxidize a wide variety of organics, namely indirect electrolysis in electrochemical oxidation. However, in electrooxidation, pollutants can be removed by (i) indirect electrolysis, and/or (ii) direct electrolysis, where pollutants exchange electrons directly with the anode surface without involvement of other substances [47,48]. Fig. 8 plots the concentration of •OH ($C_{^\bullet OH}$) in degradation solution, which depicted that $C_{^\bullet OH}$ was increased with increasing electrolysis time for all processes regardless of electrode. The $C_{^\bullet OH}$ of SnO_2-Sb/CA and SnO_2-Sb/Ti in US-EC process was respectively up to 19.3 and 10.2 μM at 2 h, increasing respectively by 54% and 22% compared to corresponding sole EC system. The prominently enhanced amount of •OH can be due to the activation effect on electrode surface with the aid of US and sonochemical effect which can split water vapor to generate •OH by high bubble vapor temperature.

Furthermore, the degradation efficiency is largely influenced and controlled by diffusion process. Thus, the diffusion coefficient of PFOA on different electrodes was calculated according to Eq. (1). In sole EC process, the diffusion coefficient was 1.83×10^{-3} and 4.9×10^{-4} $cm^2\ s^{-1}$ on SnO_2-Sb/CA and SnO_2-Sb/Ti electrodes, respectively. While in US-EC process, it was corresponding rise to 4.82×10^{-3} and 1.5×10^{-3} $cm^2\ s^{-1}$ respectively on SnO_2-Sb/CA and SnO_2-Sb/Ti electrodes. US can introduce acoustic streaming of liquid and then lead to the strong agitation on solution–solution and electrode–solution interface. Thus, the diffusion layer between electrode and bulk solution will be compressed, which can speed up the diffusion rate of contaminant from solution to electrode surface, and finally enhanced the electrochemical oxidation efficiency.

Additionally, as anticipated in the experimental part, the stability of electrode was finally tested through an accelerated service-life test, polarizing the electrode at a fixed current density (100 mA cm^{-2}) in 0.1 M H_2SO4, till deactivation. The results showed that the laboratory-prepared SnO_2-Sb/CA electrode was stable for about 6.5 h under accelerated conditions, which was 2.2 times longer than SnO_2-Sb/Ti electrode (~3 h). However, the real lifetime of this electrode would be much longer and rely on the test conditions, including current density, pH and temperature of the electrolyte. A rough estimation was derived from the method described by Hine et al. [49], which gives a simple relationship between the electrode service life (SL) and the current density (i) of $SL \sim \frac{1}{i^n}$ [49,50], where n ranges from 1.4 to 2.0. Given that n is equal to an average of 1.7 for the electrode, its service life for SnO_2-Sb/CA with a current density of 100 mA cm^{-2} in strongly acidic solutions was estimated to be approximately 521 h.

3.3. *Mechanism for efficient removing PFOA by ultrasonic electrochemical oxidation with novel SnO_2-Sb/AC electrode*

In order to elucidate the PFOA degradation mechanism in US-EC system, the intermediates obtained in solution and on electrode were respectively collected and identified by GC–MS (see Table 2). Specially, the electrodes at different reaction intervals were soaked into secondary distilled water for few hours to desorption generated intermediates, which was further extracted for analysis. As shown in Table 2, the kinds of intermediate products in SnO_2-Sb/CA and SnO_2-Sb/Ti systems are quite different. In SnO_2-Sb/CA system, during the first 0.5 h, the main products detected in

Table 2
The kinds of intermediate products obtained on electrode surface and in solution after the degradation of 100 mg L^{-1} PFOA at 0.5 and 5 h in US-EC process with SnO_2-Sb/CA and SnO_2-Sb/Ti electrodes.

Reaction area	SnO_2-Sb/CA system		SnO_2-Sb/Ti system	
	0.5 h	5 h	0.5 h	5 h
Electrode	$C_5F_{11}COO^-$	$C_5F_{11}COO^-$	n.d.[a]	n.d.[a]
Surface	$C_4F_9COO^-$	$C_4F_9COO^-$	–	–
	$C_3F_7COO^-$	$C_3F_7COO^-$	–	–
	$C_2F_5COO^-$	–	–	–
	CF_3COO^-	–	–	–
Solution	$C_5F_{11}COO^-$	$C_5F_{11}COO^-$	$C_5F_{11}COO^-$	$C_5F_{11}COO^-$
	$C_4F_9COO^-$	$C_4F_9COO^-$	$C_4F_9COO^-$	$C_4F_9COO^-$
	$C_3F_7COO^-$	$C_3F_7COO^-$	$C_3F_7COO^-$	$C_3F_7COO^-$
	–	–	$C_2F_5COO^-$	$C_2F_5COO^-$
	–	–	CF_3COO^-	CF_3COO^-

[a] Not determined.

aqueous solution were $C_5F_{11}COO^-$, $C_4F_9COO^-$, $C_3F_7COO^-$, while the products on electrode were not only included $C_5F_{11}COO^-$, $C_4F_9COO^-$, $C_3F_7COO^-$ but also contained short-chain perfluorinated carboxylic acids (PFCAs) $C_2F_5COO^-$, CF_3COO^-. The absence of short-chain PFCAs in solution was mostly due to the fact that short-chain products were strongly adsorbed by CA with high surface area and then mineralized by SnO_2-Sb catalysts before spreading to the solution, again confirming the important role of SnO_2-Sb/CA electrode. With increasing the electrolysis time to 5 h, it was interesting to find that short-chain PFCAs on electrode were completely disappeared while other detected intermediates both in solution and on electrode remained the same, suggesting the mineralization of short-chain products would be completed after 5 h electrolysis. Nevertheless, in SnO_2-Sb/Ti system, the intermediates in solution remained the same including $C_5F_{11}COO^-$, $C_4F_9COO^-$, $C_3F_7COO^-$, $C_2F_5COO^-$, CF_3COO^- during the whole degradation process, while no product was detected on electrode. This observation again implied that SnO_2-Sb/CA was an excellent electrode in EC process with the aid of US for removing PFOA in terms of outstanding adsorption and electrocatalysis ability. Compared with the degradation of PFOA reported in previous references [21,51], the intermediates of $C_6F_{13}COO^-$ was absent under ultrasonic irradiation neither in SnO_2-Sb/CA nor SnO_2-Sb/Ti system. It is likely that the energy barrier for breaking the C-C bond at the end of the carbon chain including the carboxyl group is very high, which is not favorable to form $C_6F_{13}COO^-$ [52].

On the basis of the above results, possible synergetic effect between ultrasonic electrochemical oxidation and SnO_2-Sb/CA electrode catalyst for efficiently removing PFOA was proposed as shown in Fig. 9. The cavitation bubble was firstly generated on electrode surface, which continuously interacted with ultrasonic pressure wave to cause heat with high temperature. This generated high bubble vapor temperatures can homolytically split water vapor contained within bubble to produce hydroxyl radicals (•OH). Since the excellent electroadsorption capacity of this novel SnO_2-Sb/CA electrode with high surface area, organic pollutants (PFOA and its intermediates) would be easily adsorbed and aggregated on the surface, which improved the degradation reaction but also may blocked the active catalytic sites. However, with the assistance of US, the blocked electrode surface by pollutants would be quickly cleaned and alleviated. In addition, US can improve mass transfer of pollutants which keeps on rejuvenating the electrode surface. That is to say, the efficient degradation performance was due to the combined function of CA with strong adsorption capacity, SnO_2-Sb catalyst with high electrocatalysis ability and US which can simultaneously improve diffusion process and reaction rate. Furthermore, according to the obtained observation in Table 2, PFOA decay obeyed the following pathways. In the early stage, the nonterminal C—C bonds of PFOA was attacked and the main

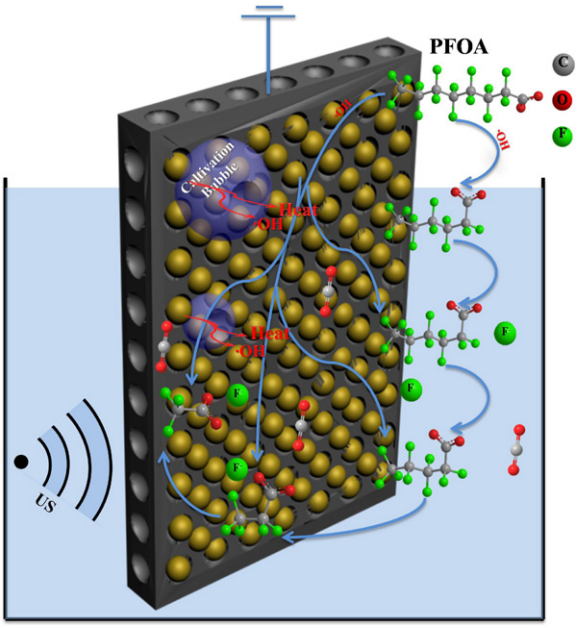

Fig. 9. Schematic mechanism for efficient decomposing PFOA by ultrasonic electrochemical oxidation with novel SnO_2-Sb/CA electrode.

generated intermediates of $C_5F_{11}COO^-$, $C_4F_9COO^-$, $C_3F_7COO^-$ were detected both on the surface of SnO_2-Sb/CA electrode and in reaction solution, while $C_2F_5COO^-$, CF_3COO^- only existed on electrode surface. In another word, PFOA was favored to be enriched on electrode surface and decomposed in EC system. Subsequently, with the eletrolysis time increased, $C_5F_{11}COO^-$, $C_4F_9COO^-$, $C_3F_7COO^-$ can be further destructed, converting into short chain PFCAs. Then CF_3COO^- can be oxidized to oxalic acid, and finally to CO_2 and H_2O, or might be directly oxidized into CO_2 and H_2O. That is why in the late reaction stage no short chain PFCAs were detected on electrode surface.

4. Conclusion

This study reported the fabrication of novel SnO_2-Sb/CA electrode catalyst and its application on degrading persistent PFOA with high concentration via ultrasonic electrochemical oxidation (US-EC) process. In order to obtain fine dispersion of Sb-doped SnO_2 active sites on CA surface and strong interaction between SnO_2-Sb and CA, the effect of heat-treating temperature was evaluated. The results revealed that the optimal calcination temperature was 600 °C for sinking micro-sized SnO_2-Sb particles existed on the surface of CA into the structure of CA as nanoparticles. The obtained SnO_2-Sb/CA electrode catalyst exhibited high surface area, strong adsorption capacity, good electrical conductivity and high degradation efficiency. Its PFOA removal and TOC removal in US-EC system was reached respectively to 91% and 86% after 5 h electrolysis, while in solo EC process the PFOA removal and TOC removal was respectively 47% and 33%. The enhanced degradation and mineralization ability with the aid of US was possible due to the increased electrocatalyst load, enhanced mass transport process, improved •OH generation and alleviated electrode surface. Moreover, substrate CA played as an important role for improving efficiency in US-EC system especially by comparing with Ti. By coupling with US, the PFOA removal with SnO_2-Sb/Ti electrode was increased from 14% to 26%, while the TOC removal was improved from 8% to 17%. In addition, the generated intermediates existed on SnO_2-Sb/CA electrode surface and in solution were respectively detected and the synergetic degradation mechanism between EC and US was

proposed. The intermediate products including ($C_5F_{11}COO^-$, $C_4F_9COO^-$, $C_3F_7COO^-$, $C_2F_5COO^-$, CF_3COO^-) were detected on electrode surface at early reaction stage (<0.5 h), and with increasing reaction time to 5 h, $C_2F_5COO^-$, CF_3COO^- were completely oxidized and then disappeared. While in solution, only $C_5F_{11}COO^-$, $C_4F_9COO^-$, $C_3F_7COO^-$ intermediates were detected during the whole reaction process, suggesting that short-chain products (C_1-C_2) would be strongly adsorbed by CA and mineralized by SnO_2-Sb before spreading into solution. For respective, this US-EC process with novel SnO_2-Sb/CA electrode catalyst has great potential to be developed as a new, simple, efficient, and promising way for the practical treatment of wastewater containing high concentration of PFOA.

Acknowledgments

This work was supported jointly by the National Natural Science Foundation P.R. China (Project NO. 21077077, 21207101), Shanghai Municipal Education Commission and Shanghai Educational Development Foundation (Project No. 2011CG19) and the Program for Young Excellent Talents in Tongji University (Project No. 2010KJ063).

References

[1] K. Prevedouros, I.T. Cousins, R.C. Buck, S.H. Korzeniowski, Environmental Science and Technology 40 (2006) 32–44.
[2] Z.M. Li, P.Y. Zhang, T. Shao, X.Y. Li, Applied Catalysis B: Environmental 125 (2012) 350–357.
[3] H. Lin, J. Niu, S. Ding, L. Zhang, Water Research 46 (2012) 2281–2289.
[4] R. Dillert, D. Bahnemann, H. Hidaka, Chemosphere 67 (2007) 785–792.
[5] H. Hori, A. Yamamoto, K. Koike, S. Kutsuna, I. Osaka, R. Arakawa, Chemosphere 68 (2007) 572–578.
[6] Z. Li, P. Zhang, T. Shao, X. Li, Applied Catalysis B: Environmental 125 (2012) 350–357.
[7] J. Cheng, D.C. Vecitis, H. Park, B.T. Mader, M.R. Hoffmann, Environmental Science and Technology 42 (2008) 8057–8063.
[8] M.H. Cao, B.B. Wang, H.S. Yu, L.L. Wang, S.H. Yuan, J. Chen, Journal of Hazardous Materials 179 (2010) 1143–1146.
[9] H. Hori, M. Murayama, N. Inoue, K. Ishida, S. Kutsuna, Catalysis Today 151 (2010) 131–136.
[10] H. Hori, Y. Nagaoka, A. Mamoto, T. Sano, N. Yamashita, S. Taniyasu, S. Kutsuna, Environmental Science and Technology 40 (2006) 1049–1054.
[11] P.J. Krusic, A.A. Marchione, D.C. Roe, Journal of Fluorine Chemistry 126 (2005) 1510–1516.
[12] C.A. Martínez-Huitle, E. Brillas, Applied Catalysis B: Environmental 87 (2009) 105–145.
[13] Q. Zhou, S. Deng, B. Yang, G. Yu, Environmental Science and Technology 45 (2011) 2973–2979.
[14] C. Pulgarin, N. Adler, P. Peringer, C. Comninellis, Water Research 28 (1994) 887–893.
[15] G. Zhao, X. Cui, M. Liu, P. Li, Y. Zhang, T. Cao, H. Li, Y. Lei, Lei, Liu, D. Li, Environmental Science and Technology 43 (2009) 1480–1486.
[16] E. Guinea, F. Centellas, E. Brillas, P. Canizares, C. Saez, M.A. Rodrigo, Applied Catalysis B: Environmental 89 (2009) 645–650.
[17] X. Zhao, J. Qu, H. Liu, Z. Qiang, R. Liu, C. Hu, Applied Catalysis B: Environmental 91 (2009) 539–545.
[18] Y. Liu, H. Liu, Y. Li, Applied Catalysis B: Environmental 84 (2008) 297–302.
[19] M. Panizza, G. Cerisola, Chemical Reviews 109 (2009) 6541–6569.
[20] S. Kim, S. Choi, B. Yoon, S. Lim, H. Park, Applied Catalysis B: Environmental 97 (2010) 135–141.
[21] H. Tang, Q. Xiang, M. Lei, J. Yan, L. Zhu, J. Zou, Chemical Engineering Journal 184 (2012) 156–162.
[22] A. Maezawa, H. Nakadoi, K. Suzuki, T. Furusawa, Y. Suzuki, S. Uchida, Ultrasonics Sonochemistry 14 (2007) 615–620.
[23] F. Trabelsi, H. Ait-Lyazidi, B. Ratsimba, A.M. Wilhelm, H. Delmas, P.L. Fabre, J. Berlan, Chemical Engineering Science 51 (1996) 1857–1865.
[24] Y.G. Adewuyi, Environmental Science and Technology 39 (2005) 3409–3420.
[25] M. Wu, Y. Jin, G. Zhao, M. Li, D. Li, Environmental Science and Technology 44 (2010) 1780–1785.
[26] Y. Jin, G. Zhao, M. Wu, Y. Lei, M. Li, X. Jin, Journal of Physical Chemistry C 115 (2011) 9917–9925.
[27] F. Montilla, E. Morallón, A.D. Battisti, J.L. Vázquez, Journal of Physics B 108 (2004) 5036–5043.
[28] L. Vazquez-Gomez, S. Ferro, A.D. Battisti, Applied Catalysis B: Environmental 67 (2006) 34–40.
[29] A. Chen, S. Nigro, Journal of Physical Chemistry B 107 (2003) 13341–13348.
[30] S. Fukui, Y. Hanasaki, H. Ogawa, Journal of Chromatography A 630 (1993) 187–193.
[31] C. Tai, J.F. Peng, J.F. Liu, G.B. Jiang, H. Zou, Analytica Chimica Acta 527 (2004) 73–80.
[32] J. Gao, G. Zhao, M. Liu, D. Li, Journal of Physical Chemistry A 113 (2009) 10466–10473.
[33] G. Zhao, S. Shen, M. Li, M. Wu, T. Cao, D. Li, Chemosphere 73 (2008) 1407–1413.
[34] L. Zhang, X. Jiang, E. Wang, S. Dong, Biosensors and Bioelectronics 21 (2005) 337–345.
[35] H. Ma, K. Teng, Y. Fu, Y. Song, Y. Wang, X. Dong, Energy & Environmental Science 4 (2011) 3067–3074.
[36] M.S. Park, G.X. Wang, Y.M. Kang, D. Wexler, S.X. Dou, H.K. Liu, Angewandte Chemie International Edition 46 (2007) 750–753.
[37] X. Chen, G. Chen, Journal of the Electrochemical Society 152 (2005) J59–J64.
[38] H.Y. Ding, Y.J. Feng, J.F. Liu, Materials Letters 61 (2007) 4920–4923.
[39] K.S.W. Sing, D.H. Everett, R.A.W. Haul, L. Moscou, R.A. Pierotti, J. Rouquerol, T. Siemieniewska, Pure & Applied Chemistry 57 (1985) 603–619.
[40] F.C. Anson, Analytical Chemistry 36 (1964) 932–934.
[41] P. Li, G. Zhao, M. Li, T. Cao, X. Cui, D. Li, Applied Catalysis B: Environmental 111–112 (2012) 578–585.
[42] X. Yang, J. Zheng, M. Zhen, X. Meng, F. Jiang, T. Wang, C. Shu, L. Jiang, C. Wang, Applied Catalysis B: Environmental 121–122 (2012) 57–64.
[43] C.D. Vecitis, Y. Wang, J. Cheng, H. Park, B.T. Mader, M.R. Hoffmann, Environmental Science and Technology 44 (2010) 432–438.
[44] M. Panizza, G. Cerisola, Chemical Reviews 109 (2009) 6541–6569.
[45] K. Ayoub, S. Nélieu, E.D. Hullebusch, J. Labanowski, I. Schmitz-Afonso, A. Bermond, M. Cassir, Applied Catalysis B: Environmental 104 (2011) 169–176.
[46] A. Ikhlaq, D.R. Brown, B. Kasprzyk-Hordern, Applied Catalysis B: Environmental 129 (2013) 437–449.
[47] E. Brillas, I. Sirés, M.A. Oturan, Chemical Reviews 109 (2009) 6570–6631.
[48] C. Comninellis, Electrochimica Acta 39 (1994) 1857–1862.
[49] F. Hine, M. Yasuda, T. Noda, T. Yoshida, J. Okuda, Journal of the Electrochemical Society 126 (1979) 1439–1445.
[50] M.H. Zhou, Q.Z. Dai, L.C. Lei, C. Ma, D.H. Wang, Environmental Science and Technology 39 (2005) 363–370.
[51] Q.F. Zhou, S.B. Deng, B. Yang, J. Huang, G. Yu, Environmental Science and Technology 45 (2011) 2973–2979.
[52] H. Xiao, B. Lv, G. Zhao, Y. Wang, M. Li, D. Li, Journal of Physical Chemistry A 115 (2011) 13836–13841.